

Application of Robust Model Predictive Control to a Renewable Hydrogen-based Microgrid

P. Velarde, J. M. Maestre, C. Ocampo-Martinez and C. Bordons

Abstract—In order to cope with uncertainties present in the renewable energy generation, as well as in the demand consumer, we propose in this paper the formulation and comparison of three robust model predictive control techniques, i.e., multi-scenario, tree-based, and chance-constrained model predictive control, which are applied to a nonlinear plant-replacement model that corresponds to a real laboratory-scale plant located in the facilities of the University of Seville. Results show the effectiveness of these three techniques considering the stochastic nature, proper of these systems.

I. INTRODUCTION

A microgrid is a small local network of electric generation that is able to integrate some renewable energy sources. Due to the intermittence in the power generation from the renewable resources, storage devices (e.g., batteries, supercapacitors, conventional capacitors, etc.) deserve special attention in the operation of this type of systems. In particular, we focus in this work on the use of hydrogen as an energy store, see, e.g., [1] and [2].

The control aim in a microgrid is to meet the consumer's demand in an optimal, economic, and safe manner despite the uncertainties that appear in the processes. Taking into account that there are mathematical models available that represent the main dynamics of these systems [3], and that the control problem requires of handling issues such as constraints, delays and disturbances, model predictive control (MPC) can be used in this context. MPC is a strategy widely used in industry for solving problems considering constraints on the manipulated and controlled variables, delays, nonlinearities, etc. The main idea of MPC is to obtain a control signal solving at each time instant an optimization problem in a finite prediction horizon based on the system model [4]. The first component of the control signal is implemented in the current time step and the problem is solved in the next time instant following a sliding time horizon strategy. Different MPC approaches have been applied in order to achieve an economical and optimal efficiency in energy management of a microgrid, see e.g., [5]–[8].

The classical formulation of MPC does not allow considering systems with uncertainties although some MPC

schemes have been proposed to ensure stability and compliance with constraints in the presence of disturbances [9]. It is worthwhile to mention that in the design of predictive controllers for dynamical systems subject to disturbances and/or uncertainty, we cannot strictly speak about feasibility but a *probability* that a certain solution is feasible.

In this paper, we use three different stochastic-programming-based MPC techniques to deal with the uncertainty of the power demand and power generation. In the first place, we consider multi-scenario MPC (MS-MPC), which consists of calculating a single control sequence that takes into account different possible evolutions of the process disturbances. Hence, the control sequence calculated has a certain degree of robustness against the possible realizations of the uncertainties. This approach is used for example in [10] in the field of control of smartgrids, and [11] for water systems. One of its advantages is that it is possible to calculate bounds on the probability of constraint violation as a function of the number of scenarios considered [12]. An alternative to model the uncertainty that is faced by this type of systems is to use rooted trees. The rationale behind this approach is that uncertainty spreads with time, i.e., it is possible to predict more accurately what the demand will be in a short horizon than in a large one. For this reason, the possible evolutions of the disturbances can be confined within a tree. Consequently, the outcome, the so called *tree-based* MPC (TB-MPC), is a rooted tree of control actions. This approach is used for example in [13] for a semi-batch reactor example and in [14] in the context of water systems. Finally, chance-constrained MPC (CC-MPC) is also studied in this work. CC-MPC uses an explicit probabilistic modeling of the system disturbances to calculate explicit bounds on the system constraint satisfaction. For instance, [15] presents chance-constrained two-stage stochastic program for unit commitment. In [16] presents a CC-MPC applied to the stock management in hospital pharmacy. An application of this technique in the context of the drinking water network (DWN) of the city of Barcelona can be seen in [17]. Also, [18] shows a comparison between TB-MPC and CC-MPC approaches applied to DWN. Further, this subject has drawn significant interest, a stochastic optimization model applied in the context of the control of microgrids, seen, e.g., [19]–[22] and references therein.

All the controllers presented in this paper have been tested with the nonlinear model of a laboratory-scale microgrid [23] and presented via simulation. The main contribution of this paper relies on the suitable review and comparison of the three proposed robust MPC techniques in order to

Financial support from the Spanish Ministry of Economy and Competitiveness (COOPERA project, under grant DPI2013-46912-C2-1-R) and the project ECOCIS (Ref. DPI2013-482443-C2-1-R) is acknowledged.

P. Velarde, J. M. Maestre and C. Bordons are with the Systems Engineering and Automatic Control Department, Universidad de Sevilla, 41092 Seville, Spain. Emails: {pabvelrue, pepemaestre, bordons}@us.es

C. Ocampo-Martinez is with Automatic Control Department, Universitat Politècnica de Catalunya, Institut de Robòtica i Informàtica Industrial (CSIC-UPC), 08028 Barcelona, Spain. E-mail: cocampo@iri.upc.edu

highlight their main advantages and weakness when coping with disturbances and uncertainties within the closed loop of a hydrogen-based microgrid.

The remainder of this paper is organized as follows. First, a description of the microgrid and its linear model are shown in Section II. Section III presents the optimization problem and the robust MPC techniques formulation. The results from simulations are shown in Section IV. Finally, in Section V, some conclusions are drawn.

II. DESCRIPTION OF THE HYLAB MICROGRID

The microgrid used is the plant developed by HyLab. The plant consists in a modular system equipped with various components that allow experimentation and simulation of various types of renewable energy sources. In Figure 1, the experimental HyLab plant is shown.

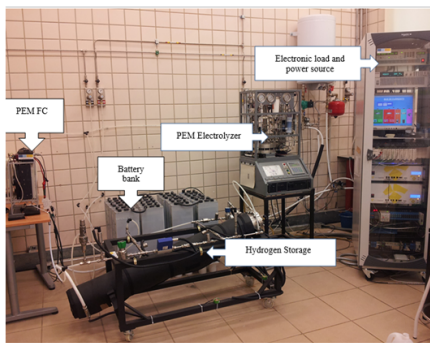


Fig. 1: Experimental HyLab Plant

The system consists of a photovoltaic field, emulated by an electronic power source, which produces electricity to supply the load. Any power excess is stored in a battery bank or derived to the electrolyzer. If the power obtained from renewable energy is not enough, both the fuel cell and the battery bank can provide power to the load, which is emulated by the electronic load source. The microgrid can work either connected to the network or as an isolated system. The Hydrogen Path is composed of two subsystems: one for producing and storing hydrogen and the other for feeding the fuel cell with hydrogen and providing power to the grid. The fuel cell and the electrolyzer are of a Proton Exchange Membrane (PEM) type and the hydrogen is stored as metal hydrides. The converters are used as power interfaces that allow the energy transfer between different devices. All units are connected via a DC bus that is regulated by the battery bank.

A. Microgrid Linear Model and Constraints

Behind the experimental setup, there is a set of nonlinear complex subsystems. The nonlinear model of the described plant, its simulation and validation are presented in [23]. In order to apply linear MPC techniques, it is necessary to take into account a linear model of the system. The linear continuous system was discretized using Tustin's method with a sampling time of 30 s.

The linear model of the plant consists of two input variables, P_{H_2} and P_{grid} , which are measured in kilowatts (kW). P_{H_2} represents the power of the electrolyzer and the power of the fuel cells: when it is greater than zero, the PEM fuel cell is working (P_{fc}) and when P_{H_2} is negative, it indicates that the electrolyzer is operating (P_{ez}). Both the electronic load and the electronic power source can either deliver or absorb power from the General Power Grid (GPG). Moreover, P_{grid} represents the power of GPG, which is positive when the power is supplied to the microgrid from the GPG and it is less than zero when delivering power to the GPG. The system is subject to disturbances (P_{net}) resulting from the difference between the power produced and the power demanded. The states are given by the state of charge of the batteries (SOC) and the metal hydrides level (MHL) of the storage tank, both measured in percentage (%). The linear model of the plant can be written as

$$x(k+1) = Ax(k) + Bu(k) + E\omega(k). \quad (1)$$

In this model, $u(k) = [P_{H_2}, P_{grid}]^T$ represents the manipulated variables; $x = [SOC, MHL]^T$ are the states of the system and $\omega(k) = P_{net}$ represents the system disturbance.

The identification process for obtaining the linear model of the plant is developed in [8].

In order to avoid damage to the equipment, it is necessary to consider limits for the Hydrogen Path operation, P_{H_2} , constraints for P_{grid} and their incremental signals ΔP_{H_2} and ΔP_{grid} , respectively, which correspond to physical limitations of the connection, i.e.,

$$-0.9 \text{ kW} \leq P_{H_2} \leq 0.9 \text{ kW}, \quad (2a)$$

$$-2.5 \text{ kW} \leq P_{grid} \leq 2 \text{ kW}, \quad (2b)$$

$$-0.9 \text{ kW} \leq \Delta P_{H_2} \leq 0.9 \text{ kW}, \quad (2c)$$

$$-2.5 \text{ kW} \leq \Delta P_{grid} \leq 2 \text{ kW}. \quad (2d)$$

Both the battery bank and the metal hydrides storage tank have limited capacity to prevent any plant damage, i.e.,

$$40\% \leq SOC \leq 90\%, \quad (3a)$$

$$10\% \leq MHL \leq 90\%. \quad (3b)$$

The input constraints given by (2) can be rewritten as

$$u(k) \in \mathcal{U}, \quad (4)$$

and the state constraints defined by (3) are expressed as

$$x(k) \in \mathcal{X}. \quad (5)$$

III. MPC IN MICROGRID HYDROGEN-BASED STORAGE

Due to the random behavior that compromises the energy generation from renewable sources and the demand consumers, the use of robust MPC techniques that account for the uncertainty is a necessity in this context, in order to meet the energy demand.

MPC is a strategy of control based on the explicit use of a dynamical model to predict the state/output of the process in future instants of time along a *prediction horizon* N . The set

of future control signals is calculated by the optimization of an objective function. Only the control signal calculated for the time instant $k \in \mathbb{Z}_+$ is applied to the process, whereas the others are discarded.

The optimization problem to solve at each time instant k is

$$\min_{u[k : k+N-1]} \sum_{i=k}^{k+N-1} J(x(i), u(i)), \quad (6)$$

subject to

$$x(i+1) = Ax(i) + Bu(i) + E, \omega(i), \quad (7a)$$

$$x(i+1) \in \mathcal{X}, \quad (7b)$$

$$u(i) \in \mathcal{U}, \quad \forall i \in \mathbb{Z}_0^{N-1}. \quad (7c)$$

The cost function that is minimized is given by

$$J(x(k), u(k)) = (x(k) - x_{\text{ref}})^T Q (x(k) - x_{\text{ref}}) + u^T(k) R u(k),$$

with $Q = 1$ and $R = [500, 600]^T$, which are weighting factors obtained after application of economic and technical criteria, given by [1]. In order to keep appropriate levels in the states of charge of the battery and the hydrogen tank, the references given are $x_{\text{ref}} = [60\%, 45\%]^T$, respectively.

The controller is designed so that the batteries are the first way of energy storage. If there exists a big difference between the demanded energy and the produced energy by the renewable sources, it proceeds to the production of hydrogen.

A. Multi-scenarios MPC approach (MS-MPC)

The optimization based on scenarios provides an intuitive way to approximate the solution to the stochastic optimization problem. To design the MS-MPC, it is enough to know several scenarios with potential evolutions of the energy demand and generation. A common control sequence that optimizes all the considered scenarios is calculated, obtaining in this way a certain robustness against the different possible evolutions of the disturbances. The scenario-based approach is computationally efficient since its solution is based on a deterministic convex optimization, even when the original problem is not [24].

The main idea for optimization considering a finite number of scenarios is to rewrite the same system for each one of known disturbances. The problem to be solved consists of

$$\min_{u[k : k+N-1]} \sum_{j=1}^K \left(\sum_{i=k}^{k+N-1} J(x_j(i), u(i)) \right), \quad (8)$$

subject to

$$x_j(i+1) = Ax_j(i) + Bu(i) + E\omega_j(i), \quad (9a)$$

$$x_j(i+1) \in \mathcal{X}, \quad \forall i \in \mathbb{Z}_0^{N-1}, \quad \forall j \in \mathbb{Z}_1^K, \quad (9b)$$

$$u(i) \in \mathcal{U}, \quad (9c)$$

where K is the number of scenarios considered.

A control sequence is optimized for the augmented system given by (9a), which includes different possible evolutions of the original one. The calculation of the controller will

result in a unique robust control action that satisfies all the potential disturbances of this extended system.

B. Tree-based MPC (TB-MPC)

This technique consists in transforming the different possible evolutions of disturbances into a rooted tree that, through its evolution, diverges and generates a reduced number of scenarios. The points of divergence are called *bifurcations* and they represent moments in time in which the evolution of the disturbances is big enough to consider more than one trajectory. The formulation of the control problem involves making tree-based optimization scenarios where only the most relevant disturbance patterns are modeled. It should be noticed that the number of scenarios used to build the tree should be in consonance with the computational capability of the controller and the probability of risk¹ in the development of the tree.

Unlike the MS-MPC problem, each scenario in the tree has its own control signal, which means that more optimization variables are needed. However, given that the control signal cannot anticipate events beyond the next bifurcation point, control sequences for different scenarios have to be equal as long as the scenarios do not branch out. As a consequence, the solution of this control problem is a rooted-tree of control actions. Notice that only the first component of this tree, which is equal for all the scenarios, is actually applied. For the design of this controller, the bifurcation points of the tree are checked: if they are equal then the control actions are the same, so that the number of variables and the calculation time can be reduced significantly.

The TB-MPC problem formulation to be solved at each time instant is represented by

$$\min_{u_j[k : k+N-1]} \sum_{j=1}^R \left(\sum_{i=k}^{k+N-1} J(x_j(i), u_j(i)) \right), \quad (10)$$

subject to

$$x_j(i+1) = Ax_j(i) + Bu_j(i) + E\omega_j(i), \quad (11a)$$

$$x_j(i+1) \in \mathcal{X}, \quad \forall i \in \mathbb{Z}_0^{N-1}, \quad (11b)$$

$$u_j(i) \in \mathcal{U}, \quad \forall j \in \mathbb{Z}_1^R, \quad (11c)$$

where R is the number of reduced scenarios from the initial K scenarios. In addition, it is necessary to introduce non-anticipative constraints to force the controller not to actuate before the uncertainty associated to the bifurcation points is solved. These constraints are given by

$$u_i(k) = u_j(k) \quad \text{if} \quad \omega_i(k) = \omega_j(k); \quad \forall i \neq j. \quad (11d)$$

As said before, a control sequence is optimized for the extended system with a disturbance tree, and only the first component of the input tree is actually applied to the system. The problem is repeated at each time instant $k \in \mathbb{Z}_+$.

¹It is the risk acceptability level of constraint violation for the states.

C. Chance-Constrained MPC (CC-MPC)

Given that disturbances have stochastic behavior, one way of addressing this problem is using CC-MPC.

The CC-MPC problem formulation is stated as

$$\min_{u[k : k+N-1]} \sum_{i=k}^{k+N-1} \mathbb{E}[J(x(i), u(i))], \quad (12)$$

subject to

$$x(i+1) = Ax(i) + Bu(i) + E\omega(i), \quad (13a)$$

$$\mathbb{P}[x_{\min} \leq x(i+1) \leq x_{\max}] > 1 - \delta_x, \quad (13b)$$

$$u(i) \in \mathcal{U}, \quad \forall i \in \mathbb{Z}_0^{N-1}, \quad (13c)$$

where $\delta_x \in (0, 1)$ is the risk of violating this constraint, x_{\min} is the lower limit and x_{\max} is the upper limit of the constrained state. Moreover, \mathbb{E} denotes the expected value of the cost function and \mathbb{P} , the probability operator.

The application of (13b) along N is necessary to implement the controller. To this end, we assume that the disturbances behave as Gaussian random variables, hence the state x is a normal variable too, with mean \bar{x} and standard deviation $\sigma_{x(k)}$, i.e., $x(k) = \mathcal{N}(\bar{x}, \sigma_{x(k)})$. The deterministic equivalent of these chance constraints can be formulated as follows:

$$\mathbb{P}(x(i+1) \geq x_{\min}) \geq 1 - \delta_x.$$

Using the change of variable, in order to standardize the normal variable

$$Z = \frac{x(i+1) - \bar{x}(i+1)}{\sigma_{x(i+1)}},$$

it is possible to write

$$\mathbb{P}(Z \geq \frac{x_{\min} - \bar{x}(i+1)}{\sigma_{x(i+1)}}) \geq 1 - \delta_x,$$

$$\mathbb{P}(Z \leq \frac{x_{\min} - \bar{x}(i+1)}{\sigma_{x(i+1)}}) \leq \delta_x,$$

$$\varphi\left(\frac{x_{\min} - \bar{x}(i+1)}{\sigma_{x(i+1)}}\right) \leq \delta_x,$$

where $\varphi(\cdot)$ is the probability distribution function. Therefore,

$$\frac{x_{\min} - \bar{x}(i+1)}{\sigma_{x(i+1)}} \leq \varphi^{-1}(\delta_x).$$

The deterministic equivalent can be written as

$$\bar{x}(i+1) \geq x_{\min} - \varphi^{-1}(\delta_x)\sigma_{x(i+1)}. \quad (14)$$

In a similar way, the upper bound of the constrained state along N can be written as

$$\bar{x}(i+1) \leq x_{\max} + \varphi^{-1}(\delta_x)\sigma_{x(i+1)}. \quad (15)$$

The expressions (14) and (15) have been formulated as the deterministic equivalent of the chance constraints.

Remark 1: The presence of the additive stochastic disturbance may lead to infeasibility when the constraints on the states and inputs, and the risk of violation of constraints are not suitably chosen. Hence, from a practical point of view, in this application the disturbance is small enough to ensure feasibility of (8), (10), and (12).

IV. RESULTS

The simulations were performed using the nonlinear model as plant replacement, see [23]. The prediction horizon was $N = 5$, the sampling time was 30 s, and the simulation period 36 hours. The linear model of the HyLab microgrid described in the Section II was used as internal model for the controller. The selected disturbance for verifying the performance of the system was the real demand registered on May 23, 2014, which is shown in Figure 2.

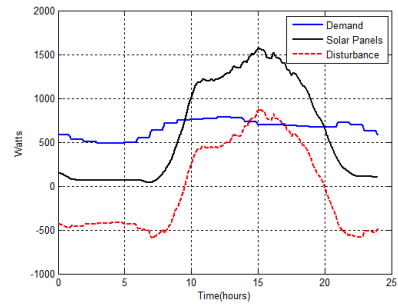


Fig. 2: Energy generated by solar panels, demand of energy and disturbance corresponding to May 23, 2014

Both, MS-MPC and TB-MPC simulations were performed by using the peninsular electricity demand and the solar generation registered by the Spanish National Electricity Network². These disturbance scenarios were the result from the difference between the electric demand and energy generated from solar-based sources at each time instant, for the months August 2013, January and April 2014. These months were chosen to have significant differences on the scenarios and all the data were scaled for the microgrid allowable values.

The MS-MPC simulations were performed considering 90 scenarios. For this number of scenarios, we expected the risk of violation of constraints according to the bound given by [24], i.e., $\delta_x < 2.2\%$. In Figure 3(a), the control signals and the disturbance are presented. In Figure 3(b), the system states are shown: the state of battery charge (SOC) and the metallic hydrides level (MHL). It can be seen in Figures 3(a) and 3(b) that the control actions drove the system towards the desired reference for each of the aforementioned states. The average tracking error of the reference to the level of battery charge (SOC) was 7.8% and metal hydride level (MHL), 2.9%. The final cumulative cost according to (8) was 1.6×10^7 .

The TB-MPC simulations were performed by using an original number of 90 scenarios, which were reduced to 5

²<https://demanda.ree.es/movil/peninsula/demanda/total>

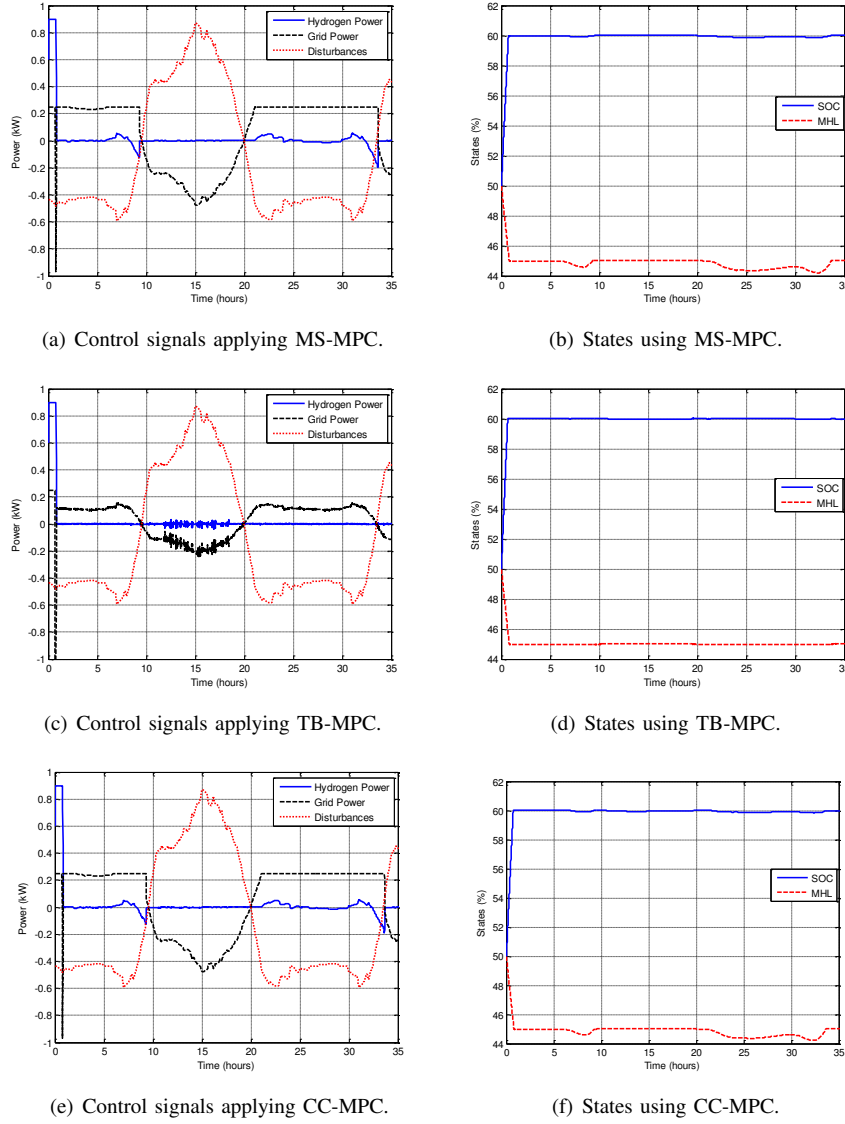


Fig. 3: Signals applying the proposed robust MPC approaches and disturbances.

scenarios forming a tree using GAMS [25] with $\delta_x < 12\%$. This reduction tried to replicate the main dynamics of all original disturbances considered in a small disturbance tree. The results are shown in Figures 3(c) and 3(d), where the control actions and system states are respectively presented.

As shown in Figures 3(c) and 3(d), the control actions satisfied the constraints of the system, driving the outputs (SOC, MHL) to the given reference. The average tracking error of the reference to the level of battery charge (SOC) was 7.72% and to the level of metallic hydrogen was 2.97%. The final cumulative cost according to (8) was 1.59×10^7 .

Simulations for CC-MPC were performed considering the failure probability $\delta_x < 1\%$. The disturbances were modeled as a normal function with $\mu = 0.3020$ and $\sigma = 0.5245$, which were obtained from the historical data registered at May 23, 2013, that is, one year ago since the simulation day. Figures 3(e) and 3(f) show that the control actions drove the

system towards the desired reference of each of the states.

The final cumulative cost was according to (8) 1.96×10^7 . The average tracking error of the reference to the level of battery charge (SOC) was 6.88% and to the level of metallic hydrogen was 2.2%.

Table I shows the average percentage error tracking the reference states, final cumulative costs, and computational times for the proposed strategies referred to the single day operation.

Figures 3(a), 3(b), referred to MS-MPC, and Figures 3(e), 3(f), carried out by CC-MPC, look very similar but the corresponding performances in Table I are quite different. On the contrary, Figures 3(c), 3(d), corresponding to TB-MPC, show a slightly different input and state behavior but the performance is similar to the one of MS-MPC. The difference between MS-MPC and CC-MPC was the computational time: the former technique worked with an

extended system while the latter only required to rewrite the constraints considering the probabilistic nature of the disturbances affecting the system. For this reason, the MS-MPC controller needed to operate with bigger matrices, which justifies its bigger computational time. The results obtained by modeling the disturbance as a tree had the minimum cost in comparison with the others but using more computational time due to it represented the disturbance scenarios into a disturbance tree at each time instant. In addition, the performance was tested with a traditional MPC, which expected a disturbance corresponding with the difference between the generation power and the demand at May 23, 2013. The robust MPC controllers provided better results with respect to the cumulative final cost, compared with a traditional MPC.

TABLE I: Cumulate final costs and average tracking errors

Approach	Final cost	SOC (%)	MHL (%)	Time (s)
MS-MPC	1.60×10^7	7.80	2.90	0.16 ± 0.01
TB-MPC	1.59×10^7	7.72	2.97	0.39 ± 0.12
CC-MPC	1.96×10^7	6.88	2.20	0.03 ± 0.01
MPC	1.90×10^8	1.50	3.60	0.16 ± 0.02

V. CONCLUSIONS

We have applied three robust MPC schemes to a microgrid based on hydrogen storage. Acting on the power of the fuel cell, electrolyzer and grid, the controllers were able to regulate the metallic hydride level and charge the battery bank to desired values. In addition, the controllers considerate constraints in both the manipulated variables and the system states for optimal performance and high functionality. As it has been seen, the system can deliver hydrogen energy once it has been stored in the form of metal hydrides to further contribute to the grid to satisfy the energy demand under the influence of uncertainties in the demand for electricity and generation.

The results obtained with the three presented versions of MPC were similar. The choice of the technique to be used will depend on the one hand if it exists a sufficient number of scenarios for considering the MS-MPC or TB-MPC, and on the other hand, if it is possible to model the disturbances as a probability distribution function for applying the CC-MPC.

REFERENCES

- [1] L. Valverde, F. Rosa, and C. Bordons. Design, planning and management of a hydrogen-based microgrid. *IEEE Transactions on Industrial Informatics*, 9(3):1398–1404, 2013.
- [2] D. Recio, C. Ocampo-Martinez, and M. Serra. Design of linear predictive controllers applied to ethanol steam reformers for hydrogen production. *International Journal of Hydrogen Energy*, 37(15):11141–11156, 2012.
- [3] T. Dragicevic, J.M. Guerrero, and J.C. Vasquez. A distributed control strategy for coordination of an autonomous LVDC microgrid based on power-line signaling. *IEEE Transactions on Industrial Electronics*, 61(7):3313–3326, 2014.
- [4] E. F. Camacho and C. Bordons. *Model Predictive Control. Second Edition*. Springer-Verlag, London, England, 2004.

- [5] P. O. Kriett and M. Salani. Optimal control of a residential microgrid. *Energy*, 42(1):321–330, 2012.
- [6] A. Parisio, E. Rikos, G. Tzamalis, and L. Glielmo. Use of model predictive control for experimental microgrid optimization. *Applied Energy*, 115:37–46, 2014.
- [7] G. Bruni, S. Cordiner, V. Mulone, V. Rocco, and F. Spagnolo. A study on the energy management in domestic micro-grids based on model predictive control strategies. *Energy Conversion and Management*, 102:50–58, 2015.
- [8] M. Pereira, D. Limón, D. Muñoz de la Peña, L. Valverde, and T. Alamo. Periodic economic control of a nonisolated microgrid. *IEEE Transactions on Industrial Electronics*, 62(8):5247–5255, 2015.
- [9] D. Bernardini and A. Bemporad. Scenario-based model predictive control of stochastic constrained linear systems. *Joint 48th IEEE Conference on Decision and Control and 28th Chinese Control Conference, Shanghai, P.R. China*, pages 6333–6338, 2009.
- [10] W. Su, J. Wang, and J. Roh. Stochastic energy scheduling in microgrids with intermittent renewable energy resources. *IEEE Transactions on Smart Grid*, 5(4):1876–1883, 2014.
- [11] P. J. van Overloop, S. Weijjs, and S. Dijkstra. Multiple model predictive control on a drainage canal system. *Control Engineering Practice*, 16(5):531–540, 2008.
- [12] G.C. Calafiore and M.C. Campi. The scenario approach to robust control design. *IEEE Transactions on Automatic Control*, 51(5):742–753, 2006.
- [13] S. Lucia, T. Finkler, D. Basak, and S. Engell. A new robust NMPC scheme and its application to a semi-batch reactor example. *In Proc. of the International Symposium on Advanced Control of Chemical Processes, Singapore*, pages 69–74, 2012.
- [14] J.M. Maestre, L. Raso, P.J. Van Overloop, and B. De Schutter. Distributed tree-based model predictive control on a drainage water system. *Journal of Hydroinformatics*, 15(2):335–347, 2013.
- [15] Q. Wang, Y. Guan, and J. Wang. A chance-constrained two-stage stochastic program for unit commitment with uncertain wind power output. *IEEE Transactions on Power Systems*, 27(1):206–215, 2012.
- [16] I. Jurado, J.M. Maestre, P. Velarde, C. Ocampo-Martinez, I. Fernández, B. Isla Tejera, and J.R. del Prado. Stock management in hospital pharmacy using chance-constrained model predictive control. *Computers in biology and medicine*, 2015 (to appear).
- [17] J.M. Grosso, C. Ocampo-Martinez, V. Puig, and B. Joseph. Chance-constrained model predictive control for drinking water networks. *Journal of Process Control*, 24(5):504–516, 2014.
- [18] J.M. Grosso, J.M. Maestre, C. Ocampo-Martinez, and V. Puig. On the assessment of tree-based and chance-constrained predictive control approaches applied to drinking water networks. *19th IFAC World Congress, Cape Town, South Africa*, pages 6240–6245, 2014.
- [19] P. Meibom, R. Barth, B. Hasche, H. Brand, C. Weber, and M. O'Malley. Stochastic optimization model to study the operational impacts of high wind penetrations in Ireland. *IEEE Transactions on Power Systems*, 26(3):1367–1379, 2011.
- [20] T.G. Hovgaard, L.F.S. Larsen, and J.B. Jorgensen. Robust economic MPC for a power management scenario with uncertainties. *In Proceedings of the 50th IEEE Conference on Decision and Control and European Control Conference (CDC-ECC), Orlando, Florida*, pages 1515–1520, 2011.
- [21] Z. Yu, L. McLaughlin, Liyan J., M.C. Murphy-Hoye, A. Pratt, and Lang T. Modeling and stochastic control for home energy management. *In Proceedings of the IEEE Power and Energy Society General Meeting*, pages 1–9, 2012.
- [22] A. Hooshmand, B. Asghari, and R. Sharma. A novel cost-aware multi-objective energy management method for microgrids. *In Proceedings of the Innovative Smart Grid Technologies (ISGT), IEEE PES, Washington, DC, USA*, pages 1–6, 2013.
- [23] L. Valverde, F. Rosa, A.J. del Real, A. Arce, and C. Bordons. Modeling, simulation and experimental set-up of a renewable hydrogen-based domestic microgrid. *International Journal of Hydrogen Energy*, 38(27):11672–11684, 2013.
- [24] G. Schildbach, L. Fagiano, C. Frei, and M. Morari. The scenario approach for stochastic model predictive control with bounds on closed-loop constraint violations. *Automatica*, 50(12):3009–3018, 2014.
- [25] A. Brooke, D. Kendrick, A. Meeraus, and R. Raman. General algebraic modeling system (GAMS): A users guide. *Boyd & Fraser publishing company, Danvers, Massachusetts*, 1988.